Sustained experimental activation of FGF8/ERK in the developing chicken spinal cord models early events in ERK-mediated tumorigenesis

Axelle Wilmerding, Lauranne Bouteille, Nathalie Caruso, Ghislain Bidaut, Heather C Etchevers, Yacine Graba, Marie-Claire Delfini

NEOPLASIA
www.neoplasia.com

Volume 24 Number xxx Month 2022 pp. 120–132

Sustained experimental activation of FGF8/ERK in the developing chicken spinal cord models early events in ERK-mediated tumorigenesis

Axelle Wilmerding [a]; Lauranne Bouteille [a]; Nathalie Caruso [a]; Ghislain Bidaut [b]; Heather C. Etchevers [c]; Yacine Graba [a,1]; Marie-Claire Delfini [a,1,2,*]

[a] Aix-Marseille Univ, CNRS, Developmental Biology Institute of Marseille (IBDM), IBDM-UMR 7288, Case 907, Parc Scientifique de Luminy, Marseille Cedex 09 13288, France
[b] INSERM, CNRS, Institut Paoli-Calmettes, CRCM, Plateform Integrative Bioinformatics, Cibi, Aix-Marseille Univ, Marseille, France
[c] Aix-Marseille Univ, INSERM, Marseille Medical Genetics, Institut MarMaRa, Marseille, France

Abstract

The MAPK/ERK pathway regulates a variety of physiological cellular functions, including cell proliferation and survival. It is abnormally activated in many types of human cancers in response to driver mutations in regulators of this pathway that trigger tumor initiation. The early steps of oncogenic progression downstream of ERK overactivation are poorly understood due to a lack of appropriate models. We show here that ERK1/2 overactivation in the trunk neural tube of the chicken embryo through expression of a constitutively active form of the upstream kinase MEK1 (MEK1ca), rapidly provokes a profound change in the transcriptional signature of developing spinal cord cells. These changes are concordant with a previously established role of the tyrosine kinase receptor ligand FGF8 acting via the ERK1/2 effectors to maintain an undifferentiated state. Furthermore, we show that MEK1ca-transfected spinal cord cells lose neuronal identity, retain caudal markers, and ectopically express potential effector oncogenes, such as AQP1. MEK1ca expression in the developing spinal cord from the chicken embryo is thus a tractable *in vivo* model to identify the mechanisms fostering neoplasia and malignancy in ERK-induced tumorigenesis of neural origins.

Neoplasia (2022) 24, 120–132

Keywords: MAPK/ERK pathway, MEK1 (MAP2K1), Developing spinal cord, Neural crest cells, Chicken embryo, Cancer model

Introduction

The spinal cord is the most caudal part of the central nervous system of vertebrates. The embryonic neural tube, from which it derives, is a pseudostratified epithelium generated progressively by neuro-mesodermal progenitors (NMP). These initially present mixed neural and mesodermal characteristics and are restricted to the most caudal part of the embryo [29,63,74]. Neurulation closely follows the caudal regression of the primitive streak and body elongation during the later stages of gastrulation. Several processes related to spinal cord specification and maturation are coupled to this caudal extension, including neurogenesis, ventral patterning, and neural crest specification; all these are regulated initially by Fibroblast Growth Factor 8 (FGF8) signaling, active in the caudal/NMP region and which maintains an undifferentiated state. Blocking FGF8 signaling in the caudal part of the embryo accelerates the onset of neural differentiation genes while ectopic maintenance of FGF8 inhibits neural differentiation [6,19,59]. This gradient of FGF8 signaling also controls progressive maturation of the paraxial mesoderm, the other major derivative of the NMP, where overexpression of FGF8 in the pre-somitic mesoderm cells prevents its differentiation and segmentation [21].

FGF signaling activates a variety of downstream effectors, including mitogen-activated protein kinases (MAPK) (extracellular signal-regulated kinases (ERK1/2)), and phosphatidylinositol 3-kinase (PI3K) [8]. During early stages of chicken embryo development, the serine/threonine kinases ERK1/2 are the main cellular effectors of FGF signaling. From the early blastula to the 10 somite stage, nearly all regions of ERK1/2 activity respond to FGF signaling [48].

The transduction of many growth factor signals including FGF into a recipient cell normally occurs through the sequential activation, by

* Corresponding author.
E-mail addresses: marie-claire.delfini-farcot@univ-amu.fr, marie-claire.delfini-farcot@sorbonne-universite.fr (M.-C. Delfini).
[1] Co-senior authors
[2] Present address: Sorbonne Université, Institut Biologie Paris Seine (IBPS), CNRS UMR7622, Developmental Biology Laboratory (LBD), Inserm U1156, F-75005 Paris, France
Received 20 September 2021; received in revised form 17 December 2021; accepted 20 December 2021

https://doi.org/10.1016/j.neo.2021.12.006

phosphorylation, of a combination of similar RAS-like GTPases, RAF and MEK enzyme family members. This process converges on the interaction of activated ERK1/2 with hundreds of cytosolic and nuclear substrates to control key cellular events including cell cycle progression, proliferation, survival and differentiation [64]. ERK1/2 overactivation in response to driver mutations in regulators of this pathway also plays an important role in the initiation and progression of most cancers [31,49]. For this reason, significant efforts have been made to develop inhibitors of RAS/ERK pathway, several of which are used in chemotherapy [64]. However, while such MAPK pathway inhibitors have improved clinical outcomes overall, emergence of drug resistance often limits their therapeutic efficacy over time [49]. It remains thus necessary to identify new targets and molecular mechanisms of oncogenic ERK1/2 activity in order to open further therapeutic perspectives. The early steps of oncogenic progression downstream of ERK1/2 overactivation are in particular poorly understood, due to a lack of appropriate in vivo models.

We used the chicken embryo to study the consequences of ERK1/2 overactivation in the developing spinal cord by expressing a constitutively active form of MEK1 (MEK1ca), the kinase just upstream of ERK1/2 [13,50]. Our results confirm previous data suggesting that the ERK1/2 pathway is the effector of FGF8 signaling in the control of neural differentiation in the spinal cord [51]. Like FGF8 gain-of-function, MEK1ca expression leads to re-expression of typical caudal genes and repression of the usual markers of the differentiating spinal cord. We furthermore showed that MEK1ca expression in the developing spinal cord rapidly and reproducibly induces neoplasia which might account from inappropriate maintenance of progenitor identity, and/or from aberrant expression of genes that could act as oncogenic downstream effectors of MAPK/ERK signalling. Since the neural tube of the trunk gives rise to both spinal cord (neurons and glia) and neural crest cells (from which in particular melanocytes and sympathetic ganglia are derived) [46], MEK1ca expression in the chicken embryo neural tube is an easily accessible *in vivo* model to identify the immediate steps downstream of MAPK/ERK signaling deregulation in oncogenic progression, relevant to a range of solid cancers including neuroblastoma, glioblastoma, and melanoma.

Results

ERK1/2 mediates FGF8 signaling to maintain undifferentiated cell states in the developing spinal cord

Inhibiting ERK1/2 activity using the MEK1/2 inhibitor PD184352 completely downregulates the expression of FGF8 target genes such as *SPRY2* in the caudal part of the chicken embryo, showing that ERK1/2 kinases are the main effectors of FGF8 in this tissue [51]. To test if maintaining ERK1/2 activity phenocopies FGF8 gain-of-function in the control of neural differentiation onset in the developing spinal cord, we electroporated the trunk neural tube of 2-day-old chicken embryos *in ovo* (Fig. 1A) with a vector expressing a constitutively active form of MEK1, a kinase encoded by the gene *MAP2K1*, directly responsible for the phosphorylation and activation of ERK1/2 ($MEK1^{\Delta N3\text{-}S218E\text{-}S222D}$ or MEK1ca [13,50]) or with a vector expressing FGF8 [14]. These vectors co-express GFP, while the control pCIG vector expresses only a nuclear-targeted form of GFP. Immunofluorescence on transverse sections with the phospho-Thr202/Tyr204-ERK1/2 (pERK) antibody one day after electroporation showed that both FGF8 and MEK1ca expression in the trunk neural tube leads to a strong increase in activated ERK1/2 signaling (Fig. 1B and Fig. S1). As shown by GFP expression, this activation was respectively indirect (non-cell-autonomous, for FGF8) or direct (cell-autonomous, for MEK1ca). Using whole-mount and transverse sections for *in situ* hybridization and immunostaining, we observed that one day after electroporation, genes expressed in the most posterior part of the neural tube (such as *SPRY2, CDX4* and *GREB1*), where ERK1/2 is activated in wild-type embryos [48], are upregulated after FGF8 and MEK1ca expression in the trunk neural tube. Conversely, genes expressed in the most anterior part of the trunk neural tube (such as *PAX6, NKX6.2* and *WNT4*) are downregulated by ectopic FGF8 and MEK1ca expression. The effect on these target transcripts was likewise long-range and non-cell autonomous for the FGF8 ligand, but cell-autonomous for MEK1ca, showing exclusion from neighboring spinal cord cells for the former and from GFP-expressing zones for the latter (Fig. 1C-D and Figs. S1-6). These results confirm the physiological function of MEK1 and ERK1/2 downstream of FGF signaling, in maintaining cells of the most caudal part of the embryo in a progenitor state during neural tube elongation and differentiation.

MEK1ca expression in the chicken neural tube leads to neoplasia

In addition to the expected developmental molecular phenotype obtained after MEK1ca transfection, which mimics at the cellular level a FGF8 gain-of-function [6,19], we found that MEK1ca leads to a profound and highly reproducible neuroepithelial disorganization observed in all MEK1ca embryos analyzed (n>100, compared to the control pCIG condition, also n >100 embryos for this study). Morphological changes in the neural tube are visible as early as one day post-electroporation, both in whole embryos examining GFP under binocular fluorescence (Fig. 2A, n>70 embryos for each condition), and on tissue sections (Fig. 2B and Fig. S7, n>15 embryos for each condition). The phenotype becomes striking by the second day after transfection, with MEK1ca-expressing cells forming disorganized aggregate structures at the transfected site (observed in all embryos analyzed, n=34 MEK1ca embryos, and never observed in pCIG embryos n=23, two or three days post-electroporation) (Fig. 2A,D,E,F and Fig. S8). MEK1ca-expressing cells also form aggregate structures at a distance from the electroporation site, particularly in the epidermis, the head, the heart, and also in the extraembryonic annexes (Fig. 2A,B,D; no distant GFP+ aggregates were observed in ten embryos transfected by pCIG (0/10), whereas five out of six MEK1ca embryos displayed distant GFP+ aggregates (5/6), with a total of eleven distant GFP+ aggregates found in these six MEK1ca embryos). F-ACTIN visualization with fluorescence-conjugated phalloidin, and immunofluorescence for a mitotic marker, pS28-H3 (pHH3), together highlighted the disorganization of the neural tube on the electroporated side of MEK1ca-transfected embryos. Mitotic cells in the MEK1ca condition are not restrained to the apical part of the future neural ependyma, as is the case in the control condition and in the contralateral part of the neural tube (Fig. 2B,C,E and Fig. S7). We found that MEK1ca expression triggers formation of rosette-like structures (Fig. 2E", F"), results in cells invading the neural tube lumen (Fig. 2F'), and favors multinucleation. Two days after electroporation, three out of five MEK1ca embryos analyzed showed multinucleated cells in the neural tube lumen (3/5), a phenotype never observed in pCIG embryos (0/5) (Fig. 2G), suggesting that induction of multinucleation by RAS/ERK overactivation [20] may be an early event during ERK-induced tumorigenesis. Cleaved caspase-3 (CASP3) immunofluorescence showed that MEK1ca expression also leads to an increase of cell death on the electroporated side (Fig. 3, see also quantification one day post-electroporation in [72]). This increase of apoptosis is consistent with previous studies showing that ERK oncogenic activity, in addition to its well-described hyperproliferative effects, also promotes apoptosis, autophagy and senescence [9]. *In situ* hybridization with a pan-neuronal *SCG10* probe (Fig. 4A), and immunostaining with antibodies against the progenitor and neuronal differentiation markers SOX2 and TUJ1, respectively, three days post-electroporation (Fig. 4B,C), showed that MEK1ca expression keeps cells in an undifferentiated state in the neural tube up to three days post-electroporation.

In conclusion, MEK1ca expression in the trunk neural tube of a two-day-old chicken embryo leads to tissue disorganization evoking neoplasia. Two days after transfection by electroporation, aggregates evocative of tumors are found not only in the neuroepithelium, i.e., at the site of the transfection, but also in adjacent and distant tissues.

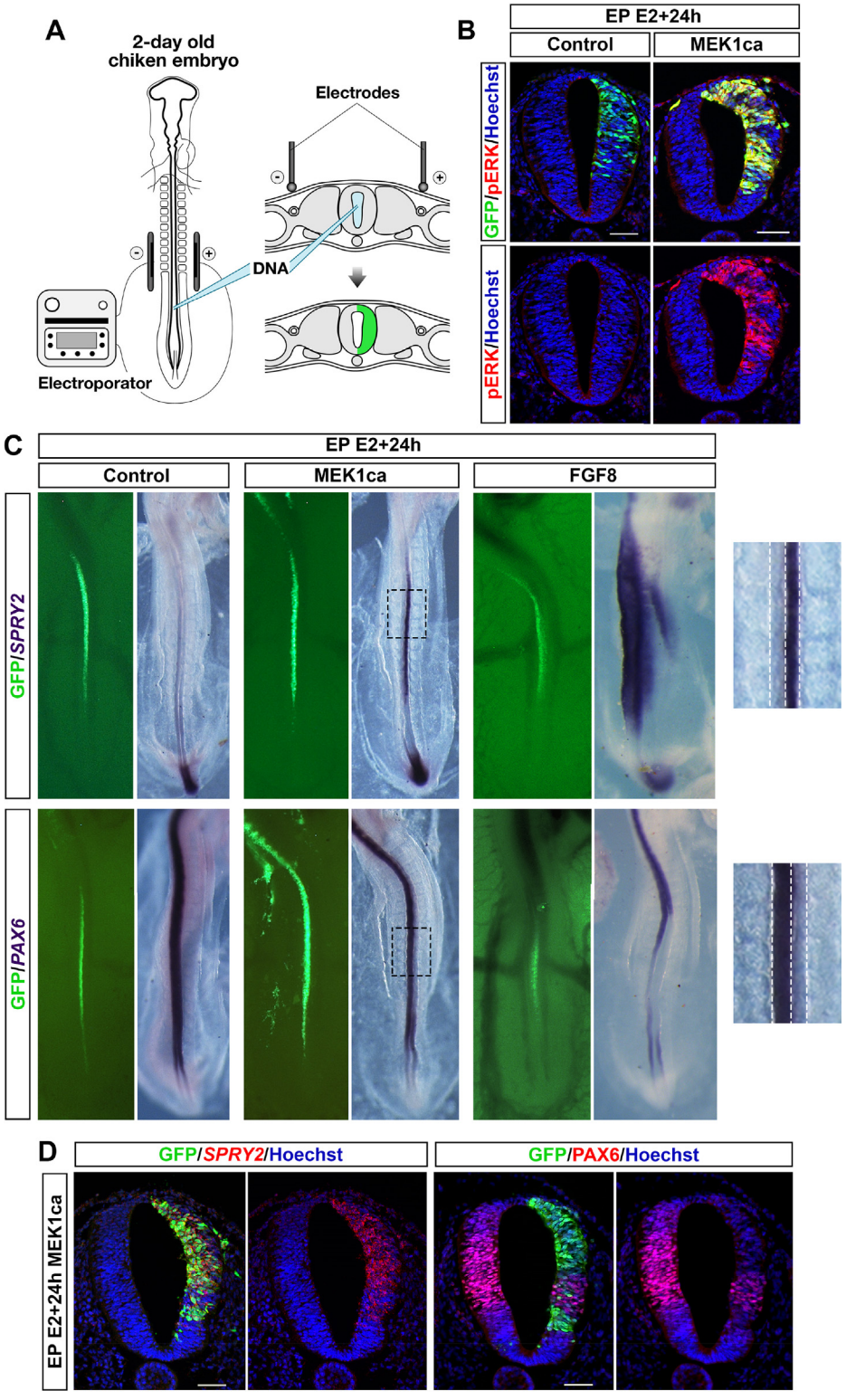

Fig. 1. MEK1ca expression phenocopies FGF8 gain-of-function in a cell-autonomous manner
A- The transfection of the neural tube of a two-day-old chicken embryo is done by unilateral or bilateral electroporation with vectors expressing GFP (control) or co-expressing GFP with MEK1ca or FGF8. **B-** Immunofluorescence on transverse sections with anti-pERK and anti-GFP antibodies one day post-electroporation with the control (pCIG) or MEK1ca-expressing vectors. **C-** Dorsal view of electroporated embryos one day post-electroporation with the control (pCIG), MEK1ca-, or FGF8-expressing vectors. Whole mount *in situ* hybridizations with SPRY2 and PAX6 probes, with corresponding GFP expression on the left. Higher magnifications of the corresponding box plot for MEK1ca condition are on the right panel **D-** Fluorescent *in situ* hybridization with SPRY2 probe and immunofluorescence using anti-GFP and anti-PAX6 antibodies on trunk-level transverse sections of a chicken embryo one day post-electroporation with the MEK1ca-expressing vector. Blue is Hoechst staining. Scale bar: 50µm.

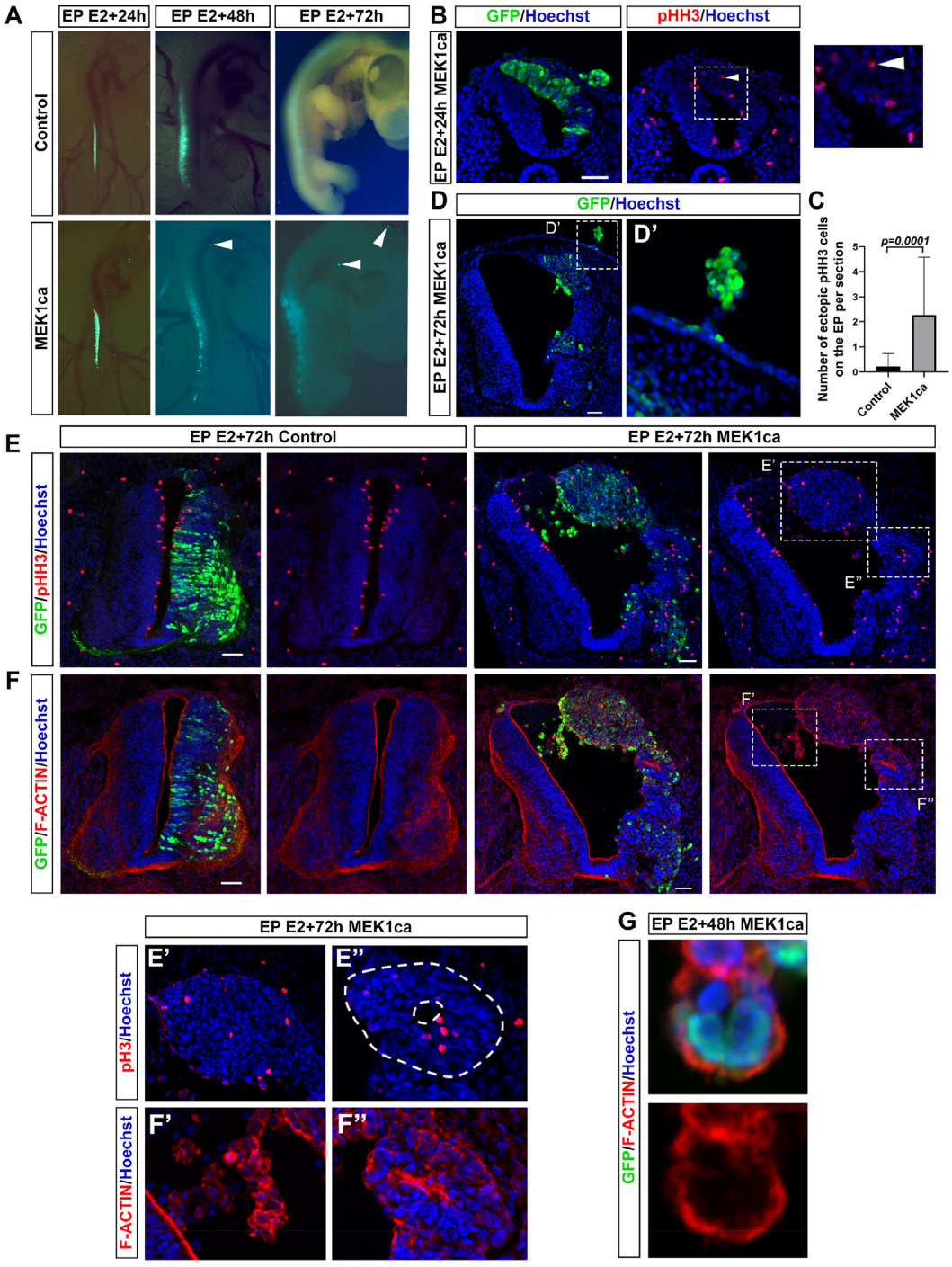

Fig. 2. MEK1ca expression in the differentiating neural tube leads to neoplasia

A- View of whole chicken embryo showing GFP fluorescence at one, two-, or three-days post-electroporation with control (pCIG) or MEK1ca-expressing vectors. White arrow heads indicate GFP+ aggregates away from the electroporated site. B- Immunofluorescence on transverse sections at the trunk level with anti-GFP and anti-pHH3 antibodies (metaphase marker) one day post-electroporation with the MEK1ca-expressing vector. **C**- The number of ectopic pHH3 cells on the electroporated side were quantified for the control (n=3, 23 sections) and MEK1ca (n=3, 26 sections). The quantification shows an increase of ectopic pHH3 cells in the electroporated side for MEK1ca embryos (two-tailed Mann–Whitney test, error bars represent s.d.). **D**- Immunofluorescence on transverse sections with anti-GFP, three days post-electroporation with the MEK1ca-expressing vector. **D'** is higher magnification within D highlighting an abnormal growth in the epidermis formed by GFP-positive cells. **E and F**- Immunofluorescence on transverse sections at 3 days post-electroporation with the PCIG (control) or MEK1ca-expressing vectors, using antibodies against GFP in conjunction with pHH3 (**E**), and F-ACTIN phalloidin staining (**F**). E' and E'' highlight ectopic mitosis both in the most dorsal part of the neural tube (**E'**) and in the rest of the tube (**E''**), forming rosette-like structures highlighted by F-ACTIN staining (**F''**). F' shows transfected cells invading the neural tube lumen. **G**- Immunofluorescence on a transverse section with anti-GFP and F-ACTIN labeling, two days post-electroporation with the MEK1ca-expressing vector, showing a cell in the lumen of the neural tube with multiple nuclei. Blue is Hoechst staining. Scale bar: 50 µm.

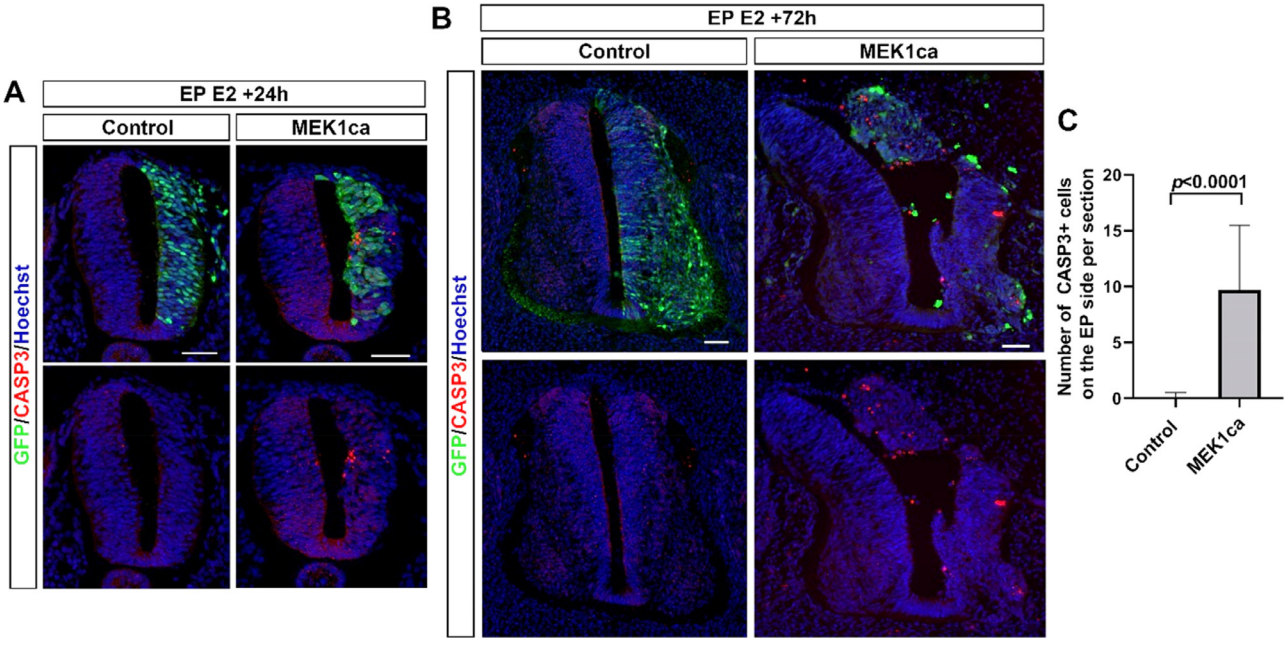

Fig. 3. The gain of function of MEK1ca induces cell death
Fluorescent immunofluorescences with anti-GFP and anti-cleaved CASP3 (apoptosis marker) antibodies on trunk transverse sections of chicken embryo (**A**) one and (**B**) three days post-electroporation with the pCIG (control) or MEK1ca expressing vectors. Blue is Hoechst staining. Scale bar: 50 µm. **C**-The number of CASP3+ cells on the electroporated side were quantified from 2 days after electroporation for the control (n=3, 35 sections) and MEK1ca (n=3, 23 sections), and the quantification shows that the gain of function of MEK1ca induces cell death (two-tailed Mann–Whitney test, error bars represent s.d.)

Transcriptomic data reproduces conclusions about the developmental function of ERK1/2 in the developing spinal cord

To further investigate the mechanisms underlying MEK1ca-induced neoplasia, we aimed to identify the global transcriptional response induced by MEK1ca in the chicken neural tube by carrying out bulk RNA-seq of GFP-positive cells from the chicken embryo neural tube one day after MEK1ca electroporation (Fig. 5A-B and Fig. S9). E2 neural tubes were bilaterally electroporated with either the control vector pCIG or the MEK1ca expression vector (Fig. 5A). Regions of the neural tube expressing GFP were dissected one day after electroporation (18-20 microdissected embryonic neural tubes by condition were pooled for each sample). After cell dissociation, GFP-expressing cells were sorted by FACS. Two independent RNA samples from GFP-expressing cells for each condition were extracted, reverse transcribed, and cDNAs were amplified using linear amplification and used for sequencing library building. After alignment to the Galgal4 genome assembly, we identified 2316 genes with significantly changed expression (Fig. 5B, Supplementary Table 1 and Supplementary Table 2; see also Material and Methods section), of which 1310 (57%) were up-regulated (Supplementary Table 1) and 1006 (43%) down-regulated (Supplementary Table 2) (Fig. 5C, top panel). By restricting to transcripts differentially expressed (DE) by more than two-fold, 348 (86 %) were up-regulated and only 57 (14 %) down-regulated (Fig. 5C, bottom panel). As expected, *SPRY2, CDX4* and *GREB1* genes are present in the list of the upregulated genes (Supplementary Table 1), and *PAX6, NKX6.2* and *WNT4* are present in the list of the downregulated genes (Supplementary Table 2). To further validate the RNAseq findings, we performed *in situ* hybridization for five additional genes found to be differentially expressed after MEK1ca expression: *CLDN1* (Fig. 5E), *IL17RD, EGR1, LIN28A* and *CHST15* (Fig. S10). All eleven DE genes examined by *in situ* hybridization after MEK1ca transfection agree with the transcriptomic data obtained by RNAseq.

Analysis of significantly over-represented biological processes using PANTHER (http://pantherdb.org/; [53]) for all the up-regulated or all the down-regulated DE genes (Fig. 5F,G and Supplementary Tables 3 and 4) highlighted the well-known autoregulatory loop of the MAPK/ERK pathway [39], cross-talk of the MAPK/ERK pathway with the PI3K pathway [75], and classical consequences of MAPK/ERK pathway activation such as the control of extra-cellular matrix synthesis and angiogenesis [17,62]. RNA-seq results were also fully consistent with the developmental function of ERK1/2 downstream of FGF8 in controlling the onset of neural differentiation in the developing spinal cord (Fig. 6A). Genes known to be endogenously expressed in the most caudal part of the embryo were upregulated (i.e. *CLDN1, DUSP5, IL17RD, DUSP4, LIN28A* and *BRA* genes in addition to *SPRY2, CDX4* and *GREB1*), while genes endogenously expressed in the differentiating neural tube were downregulated (i.e. *PLXNA2, ENPP2* and *DBX2* genes in addition to *PAX6, NKX6.2* and *WNT4*) [56] (Fig. 6B-C, Supplementary Tables 1-2).

MEK1ca induced transcriptomics evokes signatures of human central nervous system cancer cell lines

In addition to being consistent with the developmental role of ERK1/2 during the spinal cord differentiation process downstream of FGF8 signaling, our transcriptomic data showed that MEK1ca can induce the ectopic expression of genes that are neither expressed in the caudal part of the embryo nor in the neural tube at that stage normally (Fig. 6D, *e.g.* the *IL1R1, FAM65B, B3GNT7, RGS8, ARAP3, IL1RL2* and *AQP1* genes). *In situ* hybridization to *AQP1* confirmed this finding (Fig. 6E), showing ectopic expression triggered by MEK1ca in cells of the trunk neural tube, up to three days post electroporation (Fig. 6F).

Comparing the greater list of MEK1ca-deregulated genes with the ARCHS4 tissue database [45] using the "EnrichR" suite (https://maayanlab.cloud/Enrichr/; [11,44,76]) highlighted that many genes downregulated

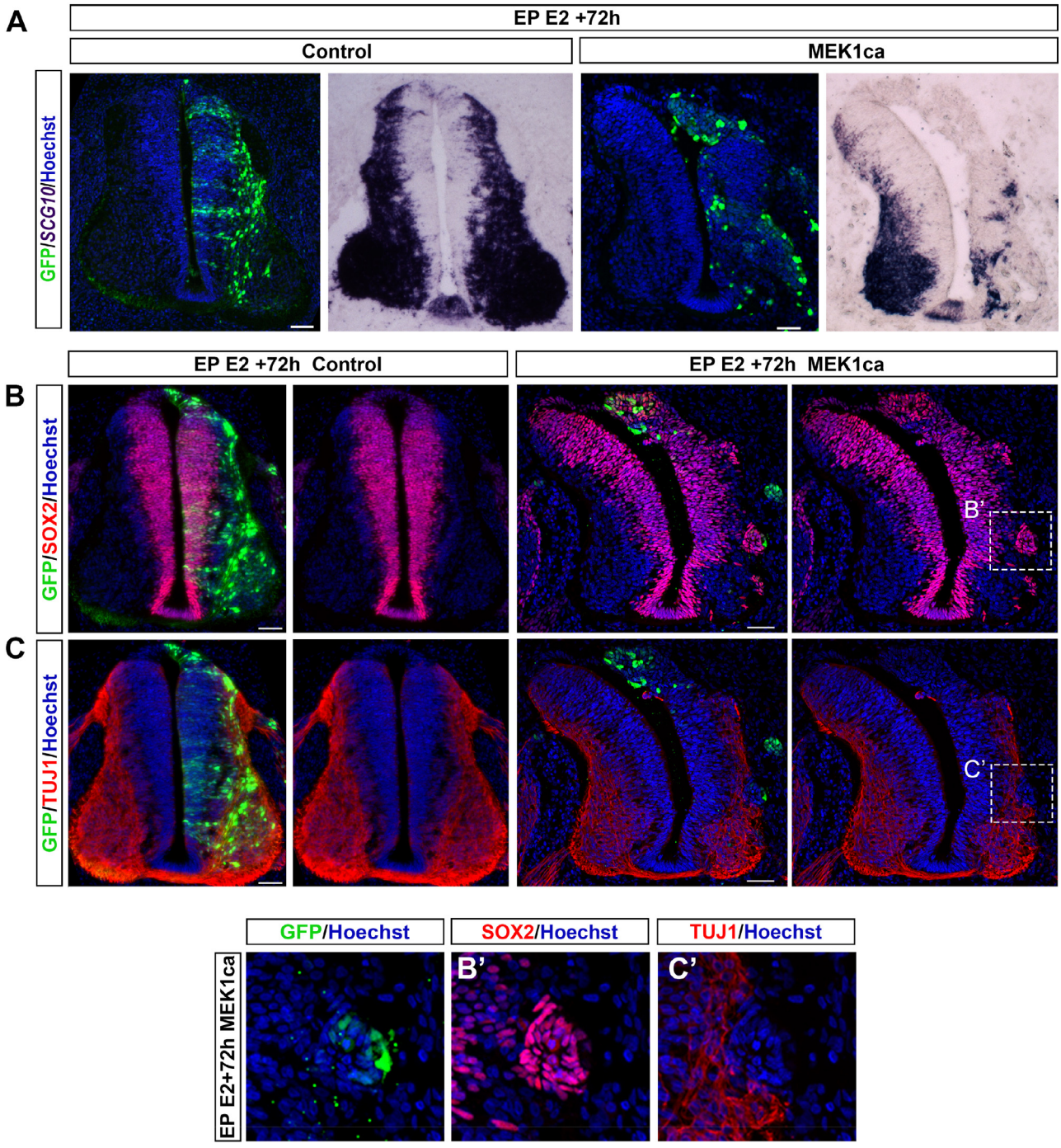

Fig. 4. The gain of function of MEK1ca prevents neuronal differentiation
A- Fluorescent *in situ* hybridization with SCG10 probe (neuronal marker) and immunofluorescences with an anti-GFP antibody. **B-** SOX2 (a neural progenitor marker) and **C-** TUJ1 (a neuronal differentiation marker) on trunk transverse sections of chicken embryo 3 days post-electroporation with the pCIG (control) or MEK1ca expressing vectors. The higher magnifications (**B'** and **C'**) are presented on the bottom panel and illustrate that the MEK1ca GFP+ cells remain SOX2+ and do not express the neuronal differentiation marker TUJ1. Blue is Hoechst. Scale bar: 50µm.

correlate with spinal cord cell-type identities (Fig. 6G, Fig. S11A). Upregulated genes found in this comparison are instead associated with terms related to fibroblasts, placenta, liver, osteoblasts, and renal tissues (Fig. 6G, Fig. S11B). These results may indicate the acquisition of aberrant cell fates, a feature of cancer cells [69], which our study further suggests may occur very early in tumorigenesis following ERK hyperactivation. Interestingly, the up-regulated gene signature of MEK1ca-expressing cells within the neural tube is consistent with the site of transfection, in that it is closer to the signature of central nervous system cancer cell lines and skin cancers than other types of cancer, when compared to transcriptomic profiles of cancer cell lines from the Broad Institute Cancer Cell Line Encyclopedia (CCLE) [4] (Fig. 6H). Strikingly, regardless of their dorso-ventral position, the transcriptional response of all neural tube cells to MEK1ca expression is homogeneous for each of the genes analyzed by *in situ* hybridization (12/12)

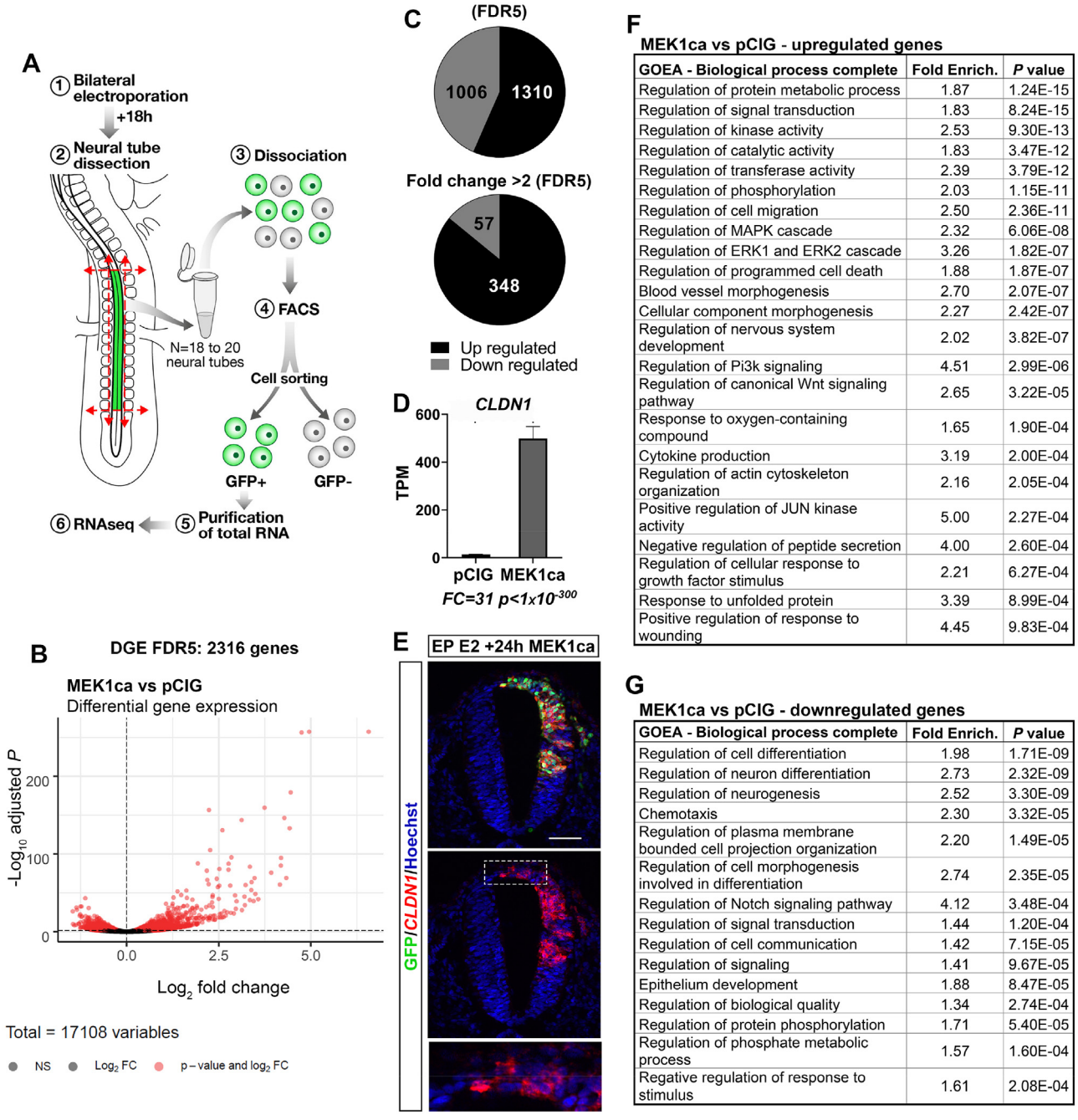

F

MEK1ca vs pCIG - upregulated genes

GOEA - Biological process complete	Fold Enrich.	*P* value
Regulation of protein metabolic process	1.87	1.24E-15
Regulation of signal transduction	1.83	8.24E-15
Regulation of kinase activity	2.53	9.30E-13
Regulation of catalytic activity	1.83	3.47E-12
Regulation of transferase activity	2.39	3.79E-12
Regulation of phosphorylation	2.03	1.15E-11
Regulation of cell migration	2.50	2.36E-11
Regulation of MAPK cascade	2.32	6.06E-08
Regulation of ERK1 and ERK2 cascade	3.26	1.82E-07
Regulation of programmed cell death	1.88	1.87E-07
Blood vessel morphogenesis	2.70	2.07E-07
Cellular component morphogenesis	2.27	2.42E-07
Regulation of nervous system development	2.02	3.82E-07
Regulation of Pi3k signaling	4.51	2.99E-06
Regulation of canonical Wnt signaling pathway	2.65	3.22E-05
Response to oxygen-containing compound	1.65	1.90E-04
Cytokine production	3.19	2.00E-04
Regulation of actin cytoskeleton organization	2.16	2.05E-04
Positive regulation of JUN kinase activity	5.00	2.27E-04
Negative regulation of peptide secretion	4.00	2.60E-04
Regulation of cellular response to growth factor stimulus	2.21	6.27E-04
Response to unfolded protein	3.39	8.99E-04
Positive regulation of response to wounding	4.45	9.83E-04

G

MEK1ca vs pCIG - downregulated genes

GOEA - Biological process complete	Fold Enrich.	*P* value
Regulation of cell differentiation	1.98	1.71E-09
Regulation of neuron differentiation	2.73	2.32E-09
Regulation of neurogenesis	2.52	3.30E-09
Chemotaxis	2.30	3.32E-05
Regulation of plasma membrane bounded cell projection organization	2.20	1.49E-05
Regulation of cell morphogenesis involved in differentiation	2.74	2.35E-05
Regulation of Notch signaling pathway	4.12	3.48E-04
Regulation of signal transduction	1.44	1.20E-04
Regulation of cell communication	1.42	7.15E-05
Regulation of signaling	1.41	9.67E-05
Epithelium development	1.88	8.47E-05
Regulation of biological quality	1.34	2.74E-04
Regulation of protein phosphorylation	1.71	5.40E-05
Regulation of phosphate metabolic process	1.57	1.60E-04
Regative regulation of response to stimulus	1.61	2.08E-04

Fig. 5. Characterization of the MEK1ca-induced transcriptome

A- One day after bilateral electroporation of the trunk neural tube at HH12 with the pCIG control or the MEK1ca vector, the electroporated region of the neural tube was dissected (18-20 embryos per condition in duplicate) and GFP-positive cells were sorted by FACS. **B-** Volcano plot of differential gene expression (DGE) for the MEK1ca versus control conditions. **C-** Pie charts representing the number of upregulated and downregulated genes in the presence of MEK1ca for FDR5 (FDR<=0.05) (all the genes) or for FDR5 and with greater than twofold change in normalized transcript numbers. **D-** Graph of *CLDN1* TPM (transcripts per kilobase million), obtained for the two replicates of the control (pCIG1, pCIG2) and MEK1ca- (MEK1ca-1 and MEK1ca-2) expressing samples, with the corresponding fold change (FC) and pvalue for MEK1ca vs pCIG. **E-** Fluorescent *in situ* hybridization with *CLDN1* probe and immunofluorescence with anti-GFP antibody on trunk-level transverse sections of a chicken embryo one day post-electroporation with the MEK1ca-expressing vector. Blue is Hoechst staining of nuclear DNA. Scale bar: 50 µm. **F-G-** Gene Ontology Enrichment Analysis (GOEA) of the biological processes for up- (**F**) and downregulated (**G**) genes in the MEK1ca versus control conditions (FDR5).

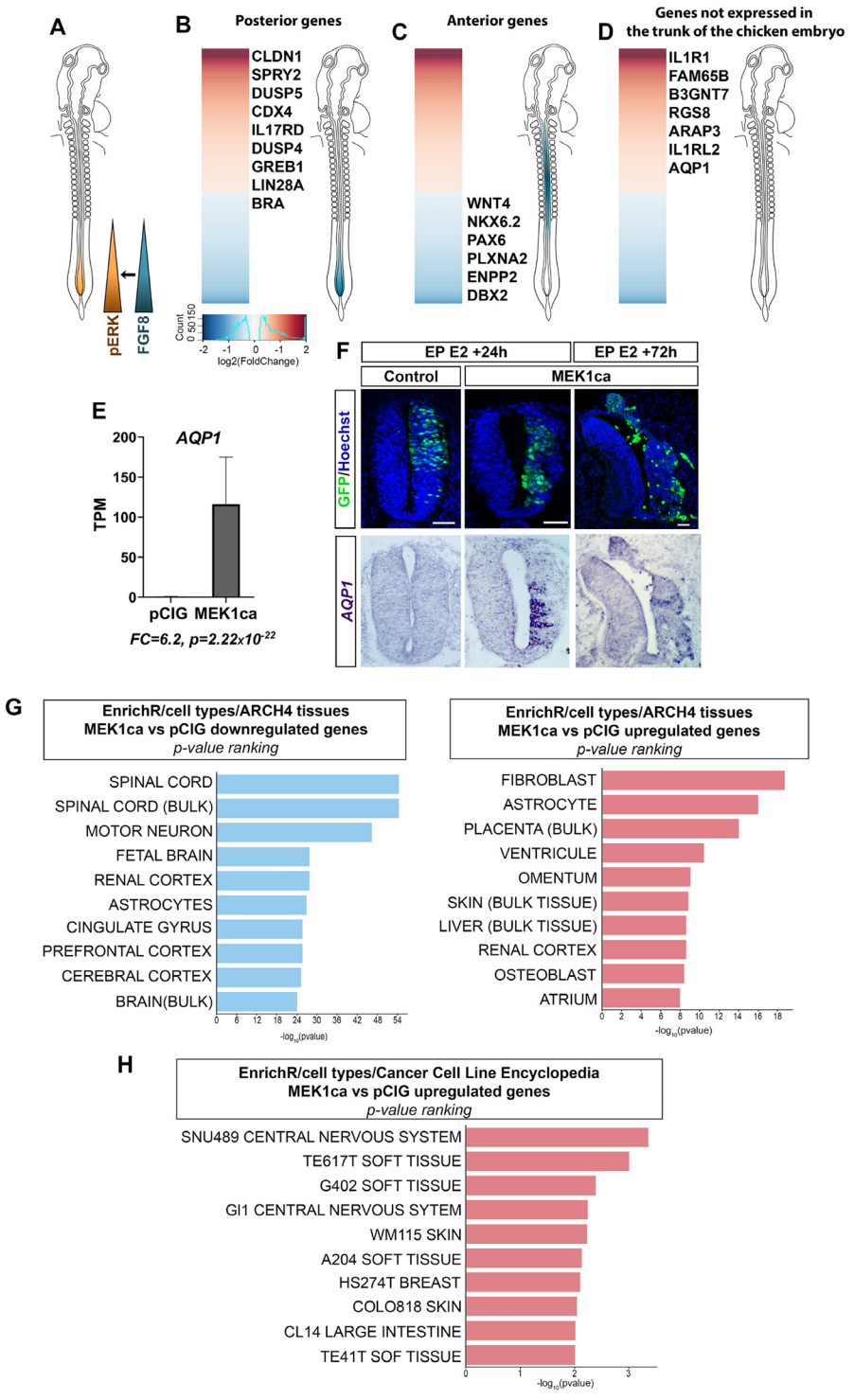

Fig. 6. Features of the MEK1ca-induced transcriptome

A- Diagram showing the expression and activation domains of FGF8 and ERK1/2 respectively in the trunk of chicken embryo at E2. **B-D-** Heat map of 2316 genes deregulated in MEK1ca-versus pCIG-transfected embryos (DGE with FDR5<=0.05) with a list of typical (**B**) posterior genes that are upregulated, (**C**) anterior genes that are downregulated, and (**D**) genes not usually expressed in the trunk of chicken embryo at that stage that are ectopically upregulated. All genes are ranked per Fold Change. **E-** Graph of the mean *AQP1* TPM (transcripts per kilobase million), obtained for the replicates of the control (pCIG1, pCIG2) and MEK1ca- (MEK1ca-1 and MEK1ca-2) expressing samples, with the corresponding fold change (FC) and pvalue for MEK1ca vs pCIG. **F-** *In situ* hybridization with *AQP1* probe and immunofluorescence using an anti-GFP antibody on trunk-level transverse sections of chicken embryos one- or three-days post-electroporation with the MEK1ca-expressing vector. Blue in top panel is Hoechst staining. Scale bar: 50 µm. **G-** Comparison of the lists of downregulated (left panel) and upregulated (right panel) genes for MEK1ca- vs pCIG-transfected neural tubes with the ARCHS4 Tissues database using the EnrichR analysis tool (2021) for cell types. **H-** Comparison of the list of upregulated genes for MEK1ca-vs pCIG-transfected neural tubes with the CCLE data base using the EnrichR analysis tool for cell types (2021).

(Figs. 1D, 5E, 6F and Figs. S3, S4 and S10), suggesting that all cell subtypes of the developing spinal cord, and neural crest cells of the trunk, which are present at the stage of the electroporation in the most dorsal part of the trunk neural tube, display the same overall transcriptional response after MEK1ca expression. The homogenous response to MEK1ca expression among the distinct cell types contained in the neural tube suggests that the ERK targets identified in this study are also likely to be relevant to cancers originating from neural crest cells, such as melanoma, as to central nervous system cancers.

Discussion

MEK1-ERK1/2 controls spinal cord differentiation downstream of FGF8 signal by maintaining caudal cells in a progenitor state

The RAS/ERK1/2 signal transduction cascade, which involves the sequential activation of RAS, RAF, MEK and ERK1/2, is a central signaling pathway that depending on the context controls cell survival and proliferation, but also cell differentiation, cell senescence, and apoptosis [16]. It is regulated by feedback loops at multiple levels, which are essential for regulating cell growth and homeostasis [22]. This pathway plays in particular critical roles during the development of the central nervous system. RAS/ERK functions in neurodevelopment are pleiotropic, ranging from promoting cell proliferation to the induction of neuronal or glial differentiation, depending on cellular context and developmental stage [32,34,47,52,55]. Activation of ERK1/2 signaling is in particular required for neural stem cells (NSCs) to maintain their ability to self-renew and to form neurospheres, indicating that ERK1/2 is a critical regulator in the maintenance of NSCs [10]. The data presented in this study are in accordance with a role for ERK1/2 activity in the maintenance of neural cells in an immature state. MEK1ca expression in the chicken embryo neural tube, which increases ERK1/2 phosphorylation and thereby activity, phenocopies at the cellular level FGF8 gain of function which maintains the cells of the developing spinal cord in a progenitor state. It was already known that FGF8/pERK1/2 downregulation acts as a switch from early (posterior) to a later (anterior) state of neural epithelial development [6,19,24,56]. We found that a few hours after electroporation, genes usually expressed in the neural tube in the most posterior part of the embryo, where ERK is physiologically activated, are upregulated by MEK1ca expression, while genes expressed in the most anterior part of the embryo are downregulated after MEK1ca transfection. Spinal cord progenitors at the level of the NMP are bipotent, since they contribute to both the spinal cord and paraxial mesoderm [70]; both lineages depend on FGF8 signaling [6,19,21,59]. As for neural differentiation of the spinal cord, ERK1/2 is the effector of the FGF8 gradient in the pre-somitic mesoderm that controls paraxial mesoderm maturation [13]. Of note, it is also *via* ERK1/2 that caudal FGF8 signaling influences the timing of neural crest cell emigration at the level of the trunk [51]. ERK1/2 is therefore the major cellular effector downstream of FGF8 signaling, orchestrating the developmental events of the caudal part of the embryo concomitantly to its extension.

The trunk neural tube of the chicken embryo is a convenient model for deciphering early events of ERK-induced tumorigenesis

In addition to its key developmental functions, the RAS/ERK1/2 pathway is intimately linked to cancer as several of its upstream activators are frequently mutated in human disease [65]. Animal models have been widely used to understand the complexity of human malignancies and in particular to establish a causal relationship between tumor development and the different MAPK/ERK pathway mutations found in human cancers. The activation of ERK1/2 in these contexts is not always clearly tumorigenic since data consistent with a role in tumor suppression have been reported as well. The intensity of ERK signaling, negative feedback loops that regulate the pathway, and cross-talk with other signaling pathways, all participate in determining the final cellular outcome [16].

The most used vertebrate animal to model tumorigenesis is the mouse. Transgenic mice expressing in different tissues mutated forms of RAS and RAF family effectors have been generated. This has allowed, for example, the modeling of pancreatic or lung cancer with oncogenic forms of *KRAF* [37]. Virus infection as well as *in utero* or postnatal electroporation are also used in mice for transduction. Notably, constitutive activation of BRAF by injection of virus-producing cells into hemispheres or brainstem of neonatal mouse can model pilocytic astrocytoma (the most common type of primary brain tumor in children and the second most frequent cancer in childhood) [27]. The zebrafish is also a powerful vertebrate model in cancer research because of its tractability for high-throughput forward genetics and chemical screens. Several transgenic zebrafish lines expressing mutated forms of RAS or RAF have been generated to model hepatocellular carcinoma [54], brain tumors [36], pancreatic cancer [58] or melanoma [60]. Zebrafish melanoma models have probed links between RAS signaling, development and cancer [1,60], discovering that reactivation of embryonic developmental pathways and modules is a critical event in melanoma initiation as well as chemotherapy resistance [38,71].

The avian model has been used for decades to study metastasis, by grafting tumor cell lines [57] or primary patient tumor cells [42] on the highly vascularized chorioallantoic membrane. Moreover, the neural tube of chicken embryo has been used to study the role of β-catenin in tumor development [30] and to model pediatric alveolar rhabdomyosarcoma, by over-expressing the chimeric PAX-FOXO1s protein [26]. To date, avian embryos have never been used to model oncogenic RAS/ERK signaling. Constitutive activation of MEK1 by expression of MEK1$^{\Delta N3\text{-}S218E\text{-}S222D}$ (MEK1ca) has long been known to massively enhance ERK1/2 phosphorylation and to promote cell transformation. Indeed, MEK1ca-expressing cells form transformed foci, grow efficiently in soft agar, and are tumorigenic when they are injected subcutaneously into the backs of weanling athymic nude mice [50]. The effect of MEK1ca expression in the embryonic chicken neural tube, where it also enhances ERK1/2 phosphorylation, expectedly induces a strong neoplastic phenotype. Serial transplantation or xenografting into recipient mice, or evidence of continuous expansion over time, would be necessary to determine whether the disseminated or localized tumors are malignant, and not only hyperproliferative, benign structures.

The major advantage of expressing MEK1ca in the chicken embryonic neural tube is that the neoplasia appears very rapidly after electroporation, directly in the cells of the tissue, and is easily accessible with minimal equipment or animal facilities. This model therefore allows access to neoplastic cells in their context, directly after ERK1/2 overactivation under convenient conditions. In addition, although numerous RAS/ERK gain-of-function vertebrate models already exist, the model we present in this study respects the 3Rs rule [68] insofar as the use of early avian embryos at the stages described here is not subject to the same constraints concerning animal experimentation in vertebrates as these alternative models.

The trunk neural tube at the stage of this study consists of a pseudostratified neuroepithelium that not only contains neural progenitors of the spinal cord (that will give rise to neurons and glial cells), but also to all the trunk neural crest cells in the most dorsal part. The neural crest cells migrate extensively to generate a prodigious number of differentiated cell types [25,46]. These cell types at the trunk level include the neurons and glial cells of the sensory, sympathetic, and parasympathetic nervous systems, and the melanocytes, the pigment-containing cells of the epidermis from which melanoma derives. Thus, targeting the trunk neural tube in 2-days old embryos allows to follow the consequences of oncogenic ERK activation *in vivo* in these different cell types simultaneously, making it possible to investigate the common and specific mechanisms of their responses to ERK1/2 overactivation. Furthermore, the trunk neural tube is a tissue very easy to manipulate and electroporate *in ovo*.

ERK1/2 transcriptional targets in the chicken developing spinal cord suggest new candidate oncogenes for neural and melanoma tumors

Activating mutations in *BRAF* are observed in many neural tumors, including pilocytic astrocytoma (PA), ganglioglioma (GG), pleomorphic xanthoastrocytoma, and glioblastoma variants [18,35,40,41,61,66]. More generally, ERK1/2 is aberrantly activated in over one-third of all human cancers and more than 90% of cutaneous melanomas [3]. In the model we present here, MEK1ca triggers aberrant expression of genes which at that stage are not expressed in the trunk of the embryo including in its most caudal part, as AQP1. MEK1ca-induced neoplasia may therefore not only be the result of inappropriate maintenance of caudal/progenitor identity, but also of aberrant induction of additional candidate oncogenes. These genes, some of which are already known to be conserved in human cancers downstream of RAS/ERK signaling like *AQP1* [33], are pertinent to human pathogenesis. Our study has generated a credible and validated list of putative oncogenes and tumor suppressors controlled at the transcriptional level by MEK1/ERK1/2 hyperactivation. This type of information is crucial for the annotations needed to conduct systems biology and further functional studies. Cellular responses to ERK1/2 in different tissues can differ greatly. However, MEK1ca triggers a broadly similar transcriptomic response throughout the neural tube along the dorso-ventral axis, despite many other genes known to be transcribed locally or in gradients at these stages. This observation suggests that at the stage of the experiment, neuronal and glial spinal cord progenitors as well as trunk neural crest cells respond mostly similarly at the transcriptomic level to ERK1/2 overactivation.

In conclusion, this study describes a new vertebrate model of neoplasia and identifies some relevant transcriptional downstream candidate effectors. Electroporation of MEK1ca into the chicken neural tube lends itself to experiments in epistasis and screening of inhibitors, as well as to teasing out interactions between converging signaling pathway, since many of the transcriptionally deregulated genes are annotated as part of the PI3K cascade. The model is also suitable to the study of the immediate post-translational modifications induced by ERK1/2 overactivation. While the tumors induced in the neural crest and tube by MEK1ca are not analogous to a single type of cancer, they do share characteristics with pediatric central nervous system tumors [43], as well as some common molecular features with two well-studied cancers of neural crest origin, i.e. melanoma [67] and neuroblastoma [7]. This novel and accessible model should help decipher the general mechanisms at work within an *in vivo* context of the oncogenic processes immediately downstream of ERK1/2 activation.

Materials and methods

Chicken embryos

Fertilized chicken eggs were obtained from EARL les Bruyères (Dangers, France) and incubated horizontally at 38°C in a humidified incubator. Embryos were staged according to the developmental table of Hamburger and Hamilton (HH) [28] or according to days of incubation (E). The chicken embryos used in this study were all in early stages of embryonic development (between E2 and E5). Therefore, no specific approval from the Institutional Animal Care and Use Committee was sought (French decree 2013-118 from 1st February 2013 and Directive 2010/63/EU (http://data.europa.eu/eli/dir/2010/63/2019-06-26) of the European Parliament and of the Council of 22 September 2010 on the protection of animals used for scientific purposes).

In ovo electroporation and plasmids

Neural tube *in ovo* electroporations were performed around HH11/12 as in [12]. Eggs were windowed, and the DNA solution was injected in the neural tube lumen. Needle L-shape platinum electrodes (CUY613P5) were placed on both sides of the embryo at the trunk level (5 mm apart), with the cathode always at its right. Five 50 ms pulses of 25 volts were given unilaterally (or bilaterally for RNAseq experiments) at 50 ms intervals with an electroporator NEPA21 (Nepagene).

The plasmids used for the gain- and loss-of-function experiments co-express a cytoplasmic or nuclear GFP (pCAGGS and pCIG respectively, used alone as controls) and the coding sequence (CDS) of the gene of interest. Vector used were: pCIG-MEK1ca (MEK1ca is human MEK1$^{\Delta N3\text{-}S218E\text{-}S222D}$ [50]) [13] and pCAGGS-FGF8 [14]. The plasmids used for electroporation were purified using the Nucleobond Xtra Midi kit (Macherey-Nagel). Final concentration of DNA delivered per embryo for electroporation is between 1 and 2 µg/µl.

Immunofluorescence and fluorescent in situ hybridization

Embryos were fixed in 4% buffered formaldehyde in PBS, then 15% and 30% sucrose in PBS, embedded in OCT (optimal cutting temperature) medium and stored at -80°C. Embryos were then sectioned into 16 µm slices with a Leica cryostat and the slides conserved at – 80°C or directly used for FISH and/or immunofluorescence.

Immunofluorescence

Slides were rehydrated in PBS then blocked with 10% goat serum, 3% BSA, 0,4% Triton X-100 in PBS for one hour. Primary antibodies were incubated overnight diluted in the same solution at 4°C. The following primary antibodies were used in this study: chicken anti-GFP 1:1000 (1020 AVES), rabbit anti-phospho-p44/42 MAPK (ERK1/2) (Thr202/Tyr204) 1:250 (Cell signaling #9101), rabbit anti-SOX2 1:500 (AB5603 Merck Millipore), mouse anti-TUJ1 1:500 (801202 Biolegend), rat anti-pHH3 1:250 (S28, Abcam ab10543), rabbit anti-cleaved-caspase 3 1:500 (Asp175, CST 9661), mouse anti-PAX6 1:500 (Developmental Studies Hybridoma Bank), Phalloidin AlexaFluor 568 1:40 (ThermoFisher). The secondary antibodies used were: anti-chicken, anti-rabbit, anti-mouse or anti-rat with conjugated fluorochromes (Alexa Fluor 488, 568 or 647; ThermoFisher) at 1:500. Sections were incubated for one hour in the blocking solution containing Hoechst dye (1:1000). Slides were washed, mounted (Thermo Scientific Shandon Immu-Mount) and imaged with a Zeiss microscope Z1 Apotome or a confocal LSM 780.

Fluorescent in situ hybridization on tissue section

The protocol for fluorescent *in situ* hybridization on tissue section is as described [15]. Briefly, slides were treated with proteinase K 10 µg/ml (3 minutes at 37°C) in a solution of Tris-HCl 50 mM pH 7.5, then in triethanolamine 0.1M and 0.25% acetic anhydride. They were pre-incubated with hybridization buffer (50% formamide, SSC 5X, Denhardt 5X, yeast tRNA 250 µg/ml and herring sperm DNA 500 µg/ml) for 3 hours at room temperature, then incubated in the same buffer with digoxygenin (DIG)-labelled RNA probes overnight at 55°C in a humid chamber. The slides were then washed twice with 0.2X SSC for 30 minutes at 65°C. After 5 minutes in TNT buffer (100 mM Tris pH7.5, 150mM NaCl and 0.1% Tween-20), they were blocked for 1 hour in buffer containing 1X TNT, 1% Blocking Reagent (BR, Merck 11096176) and 10% goat serum, then incubated in the same buffer for 3h with anti-DIG-peroxidase antibodies (1:500, Roche) and revealed using the TSA-Plus Cyanine-3 kit (Perkin- Elmer). RNA probes used for *in situ* hybridization were: *SPRY2, PAX6, NKX6.2, WNT4, GREB1, CDX4, SCG10, CLDN1*, and *AQP1*. The plasmids used to generate the *CLDN1* and *SCG10* RNA probes were kind gifts from Jean-Loup Duband and Hermann Rohrer, respectively. All the other probes were produced from PCR products amplified from cDNA of E3 chicken embryo neural tubes

(either WT or transfected by MEK1ca). PCR primer pairs used to generate the probes are listed in Supplementary Table 5.

Whole-mount in situ hybridization

The whole-mount *in situ* hybridization protocol is as described [73]. Embryos were fixed 2 hours at RT in 4% buffered formaldehyde in PBS. Embryos were dehydrated with sequential washes in 50% ethanol/ PBS+ 0.1% Tween20 then 100% ethanol and conserved at -20°C. Embryos were bleached for 45 minutes in 80% ethanol, 6% aqueous H_2O_2 and then rehydrated. They were treated 10 minutes with proteinase K 10 µg/ml at RT and refixed with 4% formaldehyde, 0.2% glutaraldehyde. After 1 hour of blocking in the hybridization buffer (50% formamide, SSC 5x, 50 μg/mL heparin, yeast tRNA 50 μg/mL, SDS 1%), hybridization with DIG-labelled RNA probes was performed at 68°C overnight. The next day, embryos were washed in hybridization buffer then once in TBS (25 mM Tris, 150 mM NaCl, 2 mM KCl, pH 7.4) + 0.1% Tween 20. They were incubated 1 hour at RT in a blocking buffer (20% Blocking Reagent [Merck/Roche] + 20% goat serum) and then overnight with an anti-DIG-AP antibody (1:2000, Merck) in the blocking buffer. After 3 washes (1 hour) in TBS+0.1% Tween 20, embryos were equilibrated in NTMT buffer (NaCl 100 mM, Tris HCl 100 mM pH 9.5, $MgCl_2$ 50 mM, 0.2% Tween-20) and incubated in NBT/BCIP (Promega) at RT in the dark until color development. Pictures of whole embryos were taken with a BinoFluo MZFLIII and a color camera.

RNA-seq analysis

Electroporations were carried out as described above with 5 bilateral pulses. Plasmid DNA concentrations were, for the control mix, pCIG at 2 µg/µl, and for the MEK1ca mix at pCIG-MEK1ca 1 µg/µl + pCIG 1µg/µl. Parts of the neural tube expressing GFP (18 to 20 embryos per condition) were microdissected one day after electroporation and dissociated with trypsin/EDTA 0.25%. A highly enriched population of GFP-expressing cells was isolated by FACS with the use of a dead cell exclusion (DCE)/discrimination dye (DAPI) to eliminate dying cells [73]. RNA was extracted (RNeasy Mini Kit), reverse transcribed with random primers and cDNA was amplified using a linear amplification system used for building sequencing libraries (done at the GATC Services from Eurofins Genomics). After adapter ligation and adapter-specific PCR amplification, libraries were sequenced on an Illumina NextSeq for a total of 50,000,000 paired end reads with 2 × 50 bp read length. Bioinformatics analyses were done using the galgal4.0 chicken genome build. Qualitative analysis of RNA-seq data from the two samples taken independently from pools of at least 18 embryos total RNA shows a high Pearson correlation score (>0,99), indicating experimental reproducibility (Fig. S9). edgeR uses the negative binomial (NB) distribution to model the read counts for each gene in each pooled sample and applies an exact likelihood ratio test. For edgeR analysis, gene counts were obtained with the HTSeq-count script [2]. Expression was considered differential at a False Discovery Rate (FDR) of less than 5% after Benjamini-Hochberg correction [5]. The RNA-seq data discussed in this publication have been deposited in NCBI's Gene Expression Omnibus [23] and are accessible through GEO Series accession number GSE182072.

Reproducibility and quantifications

All immunofluorescence and *in situ* hybridization experiments presented were repeated independently several times on whole-mount and/or sections on several different animals (summarized in Table 6). In addition, electroporated embryos were obtained from independent electroporation sessions to ensure reproducibility.

The number of embryos and sections used for quantifications are indicated in the figure legends. Quantifications were carried out using the Cell Counter tool of Fiji software (https://imagej.net/software/fiji/). The results were analyzed and plotted using Prism 8 (GraphPad software).

Declaration of competing interest

The authors declare no competing or financial interests.

Acknowledgements

We sincerely thank Dr. Andrew Saurin for his help in the RNA-seq analysis. We would like to thank Ms. Sophie Gournet (IBPS, CNRS UMR7622) for the drawings in Figs. 1,5 and 6. We are grateful to Dr. Jean-Loup Duband and Dr. Hermann Rohrer for their generous gifts of RNA probes, to Dr. Samuel Tozer for his critical reading of the manuscript, and to the Optical Imaging Platform of the IBDM. Sequencing was carried out by GATC/Eurofins Genomics. FACS experiments were undertaken with assistance from the Centre de Recherche en Cancérologie de Marseille (CRCM).

Funding

This research was funded by grants from Canceropôle PACA (grant "Emergence" n° 2015-06 to M.-C. D.), and A*MIDEX (project ANR-11-IDEX-0001-02), funded by the «Investissements d'Avenir» French Government program and managed by the French National Research Agency (ANR) Ph.D. fellowships from La Ligue contre le Cancer and the IBDM were made to A.W. Additional funding support was provided by the Association Française contre les Myopathies (H.C.E.).

Author Contribution Statement

Axelle Wilmerding: Methodology, Formal analysis, Investigation, Validation, Roles/Writing - original draft. **Lauranne Bouteille**: Formal analysis, Investigation. **Nathalie Caruso**: Formal analysis, Investigation. **Ghislain Bidaut**: Formal analysis. **Heather C. Etchevers**: Formal analysis, Roles/Writing - original draft. **Yacine Graba**: Roles/Writing - original draf, Funding acquisition. **Marie-Claire Delfini**: Conceptualization, Supervision, Methodology, Formal analysis, Investigation, Validation, Roles/Writing - original draft, Funding acquisition.

Supplementary materials

Supplementary material associated with this article can be found, in the online version, at doi:10.1016/j.neo.2021.12.006.

References

[1] Anastasaki C, Estep AL, Marais R, Rauen KA, Patton EE. Kinase-activating and kinase-impaired cardio-facio-cutaneous syndrome alleles have activity during zebrafish development and are sensitive to small molecule inhibitors. *Hum Mol Genet* 2009;**18**:2543–54.

[2] Anders S, Pyl PT, Huber W. HTSeq–a Python framework to work with high-throughput sequencing data. *Bioinformatics* 2015;**31**:166–9.

[3] Barbosa R, Acevedo LA, Marmorstein R. The MEK/ERK network as a therapeutic target in human cancer. *Mol Cancer Res* 2021;**19**:361–74.

[4] Barretina J, Caponigro G, Stransky N, Venkatesan K, Margolin AA, Kim S, Wilson CJ, Lehár J, Kryukov GV, Sonkin D, et al. The Cancer cell line encyclopedia enables predictive modelling of anticancer drug sensitivity. *Nature* 2012;**483**:603–7.

[5] Benjamini Y, Hochberg Y. Controlling the false discovery rate: a practical and powerful approach to multiple testing. *J R Stat Soc Ser B Methodol* 1995;**57**:289–300.

[6] Bertrand N, Médevielle F, Pituello F. FGF signalling controls the timing of Pax6 activation in the neural tube. *Dev Camb Engl* 2000;**127**:4837–43.

[7] Boeva V, Louis-Brennetot C, Peltier A, Durand S, Pierre-Eugène C, Raynal V, Etchevers HC, Thomas S, Lermine A, Daudigeos-Dubus E, et al. Heterogeneity of neuroblastoma cell identity defined by transcriptional circuitries. *Nat Genet* 2017;**49**:1408–13.

[8] Böttcher RT, Niehrs C. Fibroblast growth factor signaling during early vertebrate development. *Endocr Rev* 2005;**26**:63–77.

[9] Cagnol S, Chambard J-C. ERK and cell death: Mechanisms of ERK-induced cell death - apoptosis, autophagy and senescence: ERK and cell death. *FEBS J* 2010;**277**:2–21.

[10] Campos LS, Leone DP, Relvas JB, Brakebusch C, Fässler R, Suter U, ffrench-Constant C. β1 integrins activate a MAPK signalling pathway in neural stem cells that contributes to their maintenance. *Development* 2004;**131**:3433–44.

[11] Chen EY, Tan CM, Kou Y, Duan Q, Wang Z, Meirelles GV, Clark NR, Ma'ayan A. Enrichr: interactive and collaborative HTML5 gene list enrichment analysis tool. *BMC Bioinformatic* 2013;**14**:128.

[12] Delfini M-C, Duprez D. Ectopic Myf5 or MyoD prevents the neuronal differentiation program in addition to inducing skeletal muscle differentiation, in the chick neural tube. *Development* 2004;**131**:713–23.

[13] Delfini M-C, Dubrulle J, Malapert P, Chal J, Pourquie O. Control of the segmentation process by graded MAPK/ERK activation in the chick embryo. *Proc Natl Acad Sci* 2005;**102**:11343–8.

[14] Delfini M-C, De La Celle M, Gros J, Serralbo O, Marics I, Seux M, Scaal M, Marcelle C. The timing of emergence of muscle progenitors is controlled by an FGF/ERK/SNAIL1 pathway. *Dev Biol* 2009;**333**:229–37.

[15] Delfini M-C, Mantilleri A, Gaillard S, Hao J, Reynders A, Malapert P, Alonso S, François A, Barrere C, Seal R, et al. TAFA4, a Chemokine-like protein, modulates injury-induced mechanical and chemical pain hypersensitivity in mice. *Cell Rep* 2013;**5**:378–88.

[16] Deschênes-Simard X, Kottakis F, Meloche S, Ferbeyre G. ERKs in cancer: friends or foes? *Cancer Res* 2014;**74**:412–19.

[17] Dias Carvalho P, Guimarães CF, Cardoso AP, Mendonça S, Costa ÂM, Oliveira MJ, Velho S. KRAS oncogenic signaling extends beyond cancer cells to orchestrate the microenvironment. *Cancer Res* 2018;**78**:7–14.

[18] Dias-Santagata D, Lam Q, Vernovsky K, Vena N, Lennerz JK, Borger DR, Batchelor TT, Ligon KL, Iafrate AJ, Ligon AH, et al. BRAF V600E mutations are common in pleomorphic xanthoastrocytoma: diagnostic and therapeutic implications. *PLoS One* 2011;**6**:e17948.

[19] Diez del Corral R, Olivera-Martinez I, Goriely A, Gale E, Maden M, Storey K. Opposing FGF and retinoid pathways control ventral neural pattern, neuronal differentiation, and segmentation during body axis extension. *Neuron* 2003;**40**:65–79.

[20] Dikovskaya D, Cole JJ, Mason SM, Nixon C, Karim SA, McGarry L, Clark W, Hewitt RN, Sammons MA, Zhu J, et al. Mitotic stress is an integral part of the oncogene-induced senescence program that promotes multinucleation and cell cycle arrest. *Cell Rep* 2015;**12**:1483–96.

[21] Dubrulle J, McGrew MJ, Pourquié O. FGF signaling controls somite boundary position and regulates segmentation clock control of spatiotemporal hox gene activation. *Cell* 2001;**106**:219–32.

[22] Eblen ST. Extracellular-Regulated Kinases: Signaling From Ras to ERK Substrates to Control Biological Outcomes. In: *Advances in Cancer Research*. Elsevier; 2018. p. 99–142.

[23] Edgar R. Gene Expression Omnibus: NCBI gene expression and hybridization array data repository. *Nucleic Acids Res* 2002;**30**:207–10.

[24] Ekerot M, Stavridis MP, Delavaine L, Mitchell MP, Staples C, Owens DM, Keenan ID, Dickinson RJ, Storey KG, Keyse SM. Negative-feedback regulation of FGF signalling by DUSP6/MKP-3 is driven by ERK1/2 and mediated by Ets factor binding to a conserved site within the DUSP6/MKP-3 gene promoter. *Biochem J* 2008;**412**:287–98.

[25] Giovannone D, Ortega B, Reyes M, El-Ghali N, Rabadi M, Sao S, de Bellard ME. Chicken trunk neural crest migration visualized with HNK1. *Acta Histochem* 2015;**117**:255–66.

[26] Gonzalez Curto G, Der Vartanian A, Frarma YE-M, Manceau L, Baldi L, Prisco S, Elarouci N, Causeret F, Korenkov D, Rigolet M, et al. The PAX-FOXO1s trigger fast trans-differentiation of chick embryonic neural cells into alveolar rhabdomyosarcoma with tissue invasive properties limited by S phase entry inhibition. *PLOS Genet* 2020;**16**:e1009164.

[27] Gronych J, Korshunov A, Bageritz J, Milde T, Jugold M, Hambardzumyan D, Remke M, Hartmann C, Witt H, Jones DTW, et al. An activated mutant BRAF kinase domain is sufficient to induce pilocytic astrocytoma in mice. *J Clin Invest* 2011;**121**:1344–8.

[28] Hamburger V, Hamilton HL. A series of normal stages in the development of the chick embryo. *Dev Dyn* 1992;**195**:231–72.

[29] Henrique D, Abranches E, Verrier L, Storey KG. Neuromesodermal progenitors and the making of the spinal cord. *Development* 2015;**142**:2864–75.

[30] Herrera A, Saade M, Menendez A, Marti E, Pons S. Sustained Wnt/β-catenin signalling causes neuroepithelial aberrations through the accumulation of aPKC at the apical pole. *Nat Commun* 2014;**5**:4168.

[31] Hoshino R, Chatani Y, Yamori T, Tsuruo T, Oka H, Yoshida O, Shimada Y, Ari-i S, Wada H, Fujimoto J, et al. Constitutive activation of the 41-/43-kDa mitogen-activated protein kinase signaling pathway in human tumors. *Oncogene* 1999;**18**:813–22.

[32] Imamura O, Satoh Y, Endo S, Takishima K. Analysis of extracellular signal-regulated Kinase 2 function in neural stem/progenitor cells via nervous system-specific gene disruption: analysis of extracellular signal-regulated kinase 2 function in neural stem/progenitor cells via nervous system-specific gene disruption. *Stem Cells* 2008;**26**:3247–56.

[33] Imrédi E, Tóth B, Doma V, Barbai T, Rásó E, Kenessey I, Tímár J. Aquaporin 1 protein expression is associated with BRAF V600 mutation and adverse prognosis in cutaneous melanoma. *Melanoma Res* 2016;**26**:254–60.

[34] Ito H, Nakajima A, Nomoto H, Furukawa S. Neurotrophins facilitate neuronal differentiation of cultured neural stem cells via induction of mRNA expression of basic helix-loop-helix transcription factors Mash1 and Math1. *J Neurosci Res* 2003;**71**:648–58.

[35] Jones DTW, Kocialkowski S, Liu L, Pearson DM, Bäcklund LM, Ichimura K, Collins VP. Tandem duplication producing a novel oncogenic *BRAF* fusion gene defines the majority of pilocytic astrocytomas. *Cancer Res* 2008;**68**:8673–7.

[36] Ju B, Chen W, Orr BA, Spitsbergen JM, Jia S, Eden CJ, Henson HE, Taylor MR. Oncogenic KRAS promotes malignant brain tumors in zebrafish. *Mol Cancer* 2015;**14**:18.

[37] Karreth FA, Tuveson DA. Modelling oncogenic Ras/Raf signalling in the mouse. *Curr Opin Genet Dev* 2009;**19**:4–11.

[38] Kaufman CK, Mosimann C, Fan ZP, Yang S, Thomas AJ, Ablain J, Tan JL, Fogley RD, van Rooijen E, Hagedorn EJ, et al. A zebrafish melanoma model reveals emergence of neural crest identity during melanoma initiation. *Science* 2016;**351** aad2197–aad2197.

[39] Kidger AM, Keyse SM. The regulation of oncogenic Ras/ERK signalling by dual-specificity mitogen activated protein kinase phosphatases (MKPs). *Semin Cell Dev Biol* 2016;**50**:125–32.

[40] Kleinschmidt-DeMasters BK, Aisner DL, Birks DK, Foreman NK. Epithelioid GBMs show a high percentage of BRAF V600E mutation. *Am J Surg Pathol* 2013;**37**:685–98.

[41] Knobbe CB, Reifenberger J, Reifenberger G. Mutation analysis of the Ras pathway genes NRAS, HRAS, KRAS and BRAF in glioblastomas. *Acta Neuropathol. (Berl.)* 2004;**108**:467–70.

[42] Komatsu A, Matsumoto K, Saito T, Muto M, Tamanoi F. Patient derived chicken egg tumor model (PDcE Model): current status and critical issues. *Cells* 2019;**8**:440.

[43] Kram D, Henderson J, Baig M, Chakraborty D, Gardner M, Biswas S, Khatua S. Embryonal Tumors of the central nervous system in children: the era of targeted therapeutics. *Bioengineering* 2018;**5**:78.

[44] Kuleshov MV, Jones MR, Rouillard AD, Fernandez NF, Duan Q, Wang Z, Koplev S, Jenkins SL, Jagodnik KM, Lachmann A, et al. Enrichr: a comprehensive gene set enrichment analysis web server 2016 update. *Nucleic Acids Res* 2016;**44**:W90–7.

[45] Lachmann A, Torre D, Keenan AB, Jagodnik KM, Lee HJ, Wang L,

Silverstein MC, Ma'ayan A. Massive mining of publicly available RNA-seq data from human and mouse. *Nat Commun* 2018;**9**:1366.

[46] Le Douarin N, Kalcheim C. *The Neural Crest*. Cambridge University Press; 1999.

[47] Lukaszewicz A, Savatier P, Cortay V, Kennedy H, Dehay C. Contrasting effects of basic fibroblast growth factor and neurotrophin 3 on cell cycle kinetics of mouse cortical stem cells. *J Neurosci* 2002;**22**:6610–22.

[48] Lunn JS, Fishwick KJ, Halley PA, Storey KG. A spatial and temporal map of FGF/Erk1/2 activity and response repertoires in the early chick embryo. *Dev Biol* 2007;**302**:536–52.

[49] Maik-Rachline G, Seger R. The ERK cascade inhibitors: towards overcoming resistance. *Drug Resist Updat* 2016;**25**:1–12.

[50] Mansour S, Matten W, Hermann A, Candia J, Rong S, Fukasawa K, Vande Woude G, Ahn N. Transformation of mammalian cells by constitutively active MAP kinase kinase. *Science* 1994;**265**:966–70.

[51] Martínez-Morales PL, Diez del Corral R, Olivera-Martínez I, Quiroga AC, Das RM, Barbas JA, Storey KG, Morales AV. FGF and retinoic acid activity gradients control the timing of neural crest cell emigration in the trunk. *J Cell Biol* 2011;**194**:489–503.

[52] Ménard C, Hein P, Paquin A, Savelson A, Yang XM, Lederfein D, Barnabé-Heider F, Mir AA, Sterneck E, Peterson AC, et al. An essential role for a MEK-C/EBP pathway during growth factor-regulated cortical neurogenesis. *Neuron* 2002;**36**:597–610.

[53] Mi H, Muruganujan A, Casagrande JT, Thomas PD. Large-scale gene function analysis with the PANTHER classification system. *Nat Protoc* 2013;**8**:1551–66.

[54] Nguyen AT, Emelyanov A, Koh CHV, Spitsbergen JM, Parinov S, Gong Z. An inducible *kras V12* transgenic zebrafish model for liver tumorigenesis and chemical drug screening. *Dis Model Mech* 2012;**5**:63–72.

[55] Ohtsuka M, Fukumitsu H, Furukawa S. Neurotrophin-3 stimulates neurogenetic proliferation via the extracellular signal-regulated kinase pathway. *J Neurosci Res* 2009;**87**:301–6.

[56] Olivera-Martinez I, Schurch N, Li RA, Song J, Halley PA, Das RM, Burt DW, Barton GJ, Storey KG. Major transcriptome re-organisation and abrupt changes in signalling, cell cycle and chromatin regulation at neural differentiation *in vivo*. *Development* 2014;**141**:3266–76.

[57] Palmer TD, Lewis J, Zijlstra A. Quantitative analysis of cancer metastasis using an avian embryo Model. *J Vis Exp* 2011:2815.

[58] Park JT, Leach SD. Zebrafish model of *KRAS* -initiated pancreatic cancer. *Anim Cells Syst* 2018;**22**:353–9.

[59] Patel NS, Rhinn M, Semprich CI, Halley PA, Dollé P, Bickmore WA, Storey KG. FGF signalling regulates chromatin organisation during neural differentiation via mechanisms that can be uncoupled from transcription. *PLoS Genet* 2013;**9**:e1003614.

[60] Patton EE, Widlund HR, Kutok JL, Kopani KR, Amatruda JF, Murphey RD, Berghmans S, Mayhall EA, Traver D, Fletcher CDM, et al. BRAF mutations are sufficient to promote nevi formation and cooperate with p53 in the genesis of melanoma. *Curr Biol* 2005;**15**:249–54.

[61] Pfister S, Janzarik WG, Remke M, Ernst A, Werft W, Becker N, Toedt G, Wittmann A, Kratz C, Olbrich H, et al. BRAF gene duplication constitutes a mechanism of MAPK pathway activation in low-grade astrocytomas. *J Clin Invest* 2008;**118**:1739–49.

[62] Reddy KB, Nabha SM, Atanaskova N. Role of MAP kinase in tumor progression and invasion. *Cancer Metastasis Rev* 2003;**22**:395–403.

[63] Row RH, Tsotras SR, Goto H, Martin BL. The zebrafish tailbud contains two independent populations of midline progenitor cells that maintain long-term germ layer plasticity and differentiate in response to local signaling cues. *Development* 2016;**143**:244–54.

[64] Samatar AA, Poulikakos PI. Targeting RAS–ERK signalling in cancer: promises and challenges. *Nat Rev Drug Discov* 2014;**13**:928–42.

[65] Sanchez-Vega F, Mina M, Armenia J, Chatila WK, Luna A, La KC, Dimitriadoy S, Liu DL, Kantheti HS, Saghafinia S, et al. Oncogenic signaling pathways in the cancer genome Atlas. *Cell* 2018;**173**:321–37 e10.

[66] Schindler G, Capper D, Meyer J, Janzarik W, Omran H, Herold-Mende C, Schmieder K, Wesseling P, Mawrin C, Hasselblatt M, et al. Analysis of BRAF V600E mutation in 1,320 nervous system tumors reveals high mutation frequencies in pleomorphic xanthoastrocytoma, ganglioglioma and extra-cerebellar pilocytic astrocytoma. *Acta Neuropathol (Berl)* 2011;**121**:397–405.

[67] Shakhova O. Neural crest stem cells in melanoma development. *Curr Opin Oncol* 2014;**26**:215–21.

[68] Sneddon LU, Halsey LG, Bury NR. Considering aspects of the 3Rs principles within experimental animal biology. *J Exp Biol* 2017;**220**:3007–16.

[69] Suzuki A, Makinoshima H, Wakaguri H, Esumi H, Sugano S, Kohno T, Tsuchihara K, Suzuki Y. Aberrant transcriptional regulations in cancers: genome, transcriptome and epigenome analysis of lung adenocarcinoma cell lines. *Nucl Acids Res* 2014;**42**:13557–72.

[70] Tzouanacou E, Wegener A, Wymeersch FJ, Wilson V, Nicolas J-F. Redefining the progression of lineage segregations during mammalian embryogenesis by clonal analysis. *Dev Cell* 2009;**17**:365–76.

[71] White RM, Cech J, Ratanasirintrawoot S, Lin CY, Rahl PB, Burke CJ, Langdon E, Tomlinson ML, Mosher J, Kaufman C, et al. DHODH modulates transcriptional elongation in the neural crest and melanoma. *Nature* 2011;**471**:518–22.

[72] Wilmerding A, Bouteille L, Rinaldi L, Caruso N, Graba Y, Delfini M-C. HOXB8 counteracts MAPK/ERK oncogenic signaling in a chicken embryo model of neoplasia. *Int J Mol Sci* 2021;**22**:8911.

[73] Wilmerding A, Rinaldi L, Caruso N, Lo Re L, Bonzom E, Saurin AJ, Graba Y, Delfini M-C. HoxB genes regulate neuronal delamination in the trunk neural tube by controlling the expression of *Lzts1*. *Development* 2021;**148**:dev195404.

[74] Wilson V, Olivera-Martinez I, Storey KG. Stem cells, signals and vertebrate body axis extension. *Development* 2009;**136**:1591–604.

[75] Won J-K, Yang HW, Shin S-Y, Lee JH, Heo WD, Cho K-H. The crossregulation between ERK and PI3K signaling pathways determines the tumoricidal efficacy of MEK inhibitor. *J Mol Cell Biol* 2012;**4**:153–63.

[76] Xie Z, Bailey A, Kuleshov MV, Clarke DJB, Evangelista JE, Jenkins SL, Lachmann A, Wojciechowicz ML, Kropiwnicki E, Jagodnik KM, et al. Gene set knowledge discovery with Enrichr. *Curr Protoc* 2021;**1**.